BLED WORKSHOPS
IN PHYSICS
VOL. 12, NO. 1
p. 73

Proceedings of the Mini-Workshop
Understanding hadronic spectra
Bled, Slovenia, July 3 - 10, 2011

Scattering phase shift and resonance properties*

S. Prelovšek[a,b], C. B. Lang[c] and D. Mohler[d]

[a] J. Stefan Institute, Jamova 39, 1000 Ljubljana, Slovenia
[b] Department of Physics, University of Ljubljana, Jadranska 19, 1000 Ljubljana, Slovenia
[c] Institut für Physik, FB Theoretische Physik, Universität Graz, A-8010 Graz Austria
[d] TRIUMF, 4004 Wesbrook Mall Vancouver, BC V6T 2A3, Canada

Abstract. We describe the method for extracting the elastic scattering phase shift from a lattice simulation at an introductory level, for non-lattice practitioners. We consider the scattering in a resonant channel, where the resulting phase shift $\delta(s)$ allows the lattice determination of the mass and the width of the resonance from a Breit-Wigner type fit. We present the method for the example of P-wave $\pi\pi$ scattering in the ρ meson channel.

1 Introduction

The determination of the strong decay width of a hadronic resonance in lattice QCD is a much more demanding task than the determination of its approximate mass. The only available method (that was applied up to now) was proposed by Lüscher [1] and is rather indirect. It applies for the case when the resonance appears in the elastic scattering of two hadrons $H_1H_2 \to R \to H_1H_2$.

- First, the energy spectrum E_n of the system of two interacting hadrons H_1H_2 enclosed in a few-fermi box has to be determined. The system is illustrated in Fig. 1. The spectrum in a finite box E_n is discrete and few (one or two) lowest energy levels have to be determined by lattice simulation.
- The shift of the energy E_n with respect to the non-interacting energy $E_{H1}(\mathbf{p_1})+E_{H2}(\mathbf{p_2})$ ($E_{Hi}(\mathbf{p_i}) = \sqrt{m_i^2 + \mathbf{p_i}^2}$) gives info on the interaction between H_1 and H_2. Lüscher derived a rigorous relation between the energy shift $E_n - E_{H1} - E_{H2}$ and the elastic phase shift $\delta(s)$ for H_1H_2 scattering in continuum [1]. The measured energies E_n can be used to extract the phase shift $\delta(s)$ evaluated at $s = E_n^2 - \mathbf{P}^2$, where E_n is the energy of the system and $\mathbf{P}$ its total momentum. In order to extract $\delta(s)$ at several different values of s, the simulations are done for several choices of total momenta $\mathbf{P}$ of the H_1H_2 system, which leads to different values of $s = E_n^2 - \mathbf{P}^2$.
- The resulting dependence of $\delta(s)$ as a function of s can be used to extract the mass m_R and the width Γ_R of the resonance R, which appears in the elastic channel $H_1H_2 \to R \to H_1H_2$. For this purpose, the $\delta(s)$ can be fitted with a Breit-Wigner form or some other phenomenologically inspired form, which depend on m_R and Γ_R.

* Talk delivered by S. Prelovšek

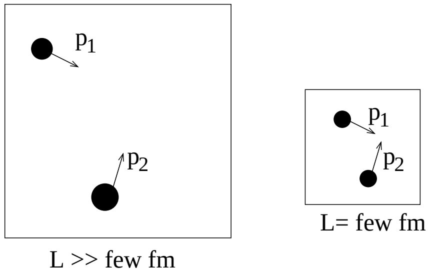

Fig. 1. The energy of two hadrons in a box of size L. On the left, $L \gg$ fm and $E(L) \simeq E_{H1}(\mathbf{p_1}) + E_{H2}(\mathbf{p_2})$. On the right, $L \simeq$ few fm and energy gets shifted due to their interaction, i.e. $E(L) \simeq E_{H1}(\mathbf{p_1}) + E_{H2}(\mathbf{p_2}) + \Delta E(L)$.

The described method, needed for the determination of the resonance width Γ_R, is rather challenging. It requires very accurate determination of a few lowest energy levels of the system H_1H_2, since the resulting phase shift depends ultimately on the energy shift. Among all the meson resonances, this method has been up to now rigorously applied only to ρ resonance. Although Lüscher proposed the method already in late 80's [1], the first lattice attempt to employ it to hadronic resonances had to wait until 2007 [2]. Since then, several studies of ρ have been carried out [3,4], with the most up to date ones [5–7].

This talk briefly describes the method to extract $\delta(s)$, m_R and Γ_R on an example of $\pi\pi$ scattering in the ρ channel. It is based on a recent simulation [6], which is the statistically most accurate determination of any strong meson width on one lattice ensemble. The purpose of this talk is to highlight the main physical reasoning, which lies behind the lattice extraction of $\delta(s)$, m_R and Γ_R, omitting most of technical details.

The sections follow the order of steps required, which are listed as items in the introduction. Section II describes the determination of spectrum E_n of the coupled system $H_1H_2 \leftrightarrow R$. The Section III described why E_n allow one to extract the elastic phase shift $\delta(s)$. The extraction of the resonance parameters m_R and Γ_R from the phase shift $\delta(s)$ is done in Section IV. We end with conclusions.

2 Spectrum of two hadrons in a finite box

The ρ meson is a resonance in $\pi\pi$ scattering in P-wave, and has quantum numbers $I^G(J^{PC}) = 1^+(1^{--})$. The total momentum $\mathbf{P}$ of the coupled $\pi\pi - \rho$ system can have values $\frac{2\pi}{N_L}\mathbf{d}$, $d \in Z^3$ due to the periodic boundary condition in the spatial direction, and we use the following three choices

$$\mathbf{P} = (0,0,0)\ ,\ \tfrac{2\pi}{N_L}(0,0,1)\ ,\ \tfrac{2\pi}{N_L}(1,1,0) \quad \text{and permutations}\ . \tag{1}$$

This enables us to obtain several values of $s = E_n^2 - \mathbf{P}^2$ for the system, thereby allowing the determination of $\delta(s)$ for these values of s without changing the spatial volume.

Our simulation is performed on an ensemble of 280 [8] gauge configurations with dynamical u/d quarks, where the valence and dynamical quarks employ improved Wilson-Clover action. The corresponding pion mass is $m_\pi a = 0.1673 \pm 0.0016$ or $m_\pi = 266 \pm 4$ MeV. The lattice spacing is $a = 0.1239 \pm 0.0013$ fm and we employ a rather small volume $N_L^3 \times N_T = 16^3 \times 32$, which allows us to use the costly full distillation method [9] for evaluating the quark contractions.

On the lattice, the discrete energies of the system E_n can be extracted after computing the dependence of the correlation matrix $C_{ij}(t_f, t_i)$ on Euclidean time $t_f - t_i$

$$C_{ij}(t_f, t_i) = \langle 0|\mathcal{O}_i(t_f)\, \mathcal{O}_j^\dagger(t_i)|0\rangle = \sum_n \langle \mathcal{O}_i|n\rangle\langle n|\mathcal{O}_j^\dagger\rangle\, e^{-E_n(t_f - t_i)}\,. \quad (2)$$

The analytical expression on the right is obtained by inserting the complete set $\sum_n |n\rangle\langle n|$ of physical states n with given quantum numbers. The interpolators O_i have the quantum numbers of the system in question. In our case the interpolators have quantum numbers $J^{PC} = 1^{--}$ and $|I, I_3\rangle = |1, 0\rangle$ and total three-momentum $\mathbf{P}$. They have to couple well to the $\pi\pi$ state and the quark-antiquark resonance ρ.

For each choice of $\mathbf{P}$ (1), we use 16 interpolators, listed in detail in Eq. (21) of [6]. We employ fifteen interpolators of quark-antiquark type

$$\mathcal{O}_i^{\bar{q}q}(t) = \sum_{\mathbf{x}} e^{i\mathbf{P}\mathbf{x}}\, \tfrac{1}{\sqrt{2}}[\bar{u}\mathcal{F}_i u\,(t, \mathbf{x}) \;+\; \bar{d}\mathcal{F}_i d\,(t, \mathbf{x})]\,, \quad (3)$$

where $\mathcal{F}_i$ denotes different color-spin-space structures with the same resulting quantum number $J^{PC} = 1^{--}$ and $|I, I_3\rangle = |1, 0\rangle$. We use also one $\pi(\mathbf{p_1})\pi(\mathbf{p_2})$ interpolator, where each pion is projected to a definite momentum

$$\begin{aligned}\mathcal{O}^{\pi\pi}(t) &= \tfrac{1}{\sqrt{2}}[\pi^+(\mathbf{p_1})\pi^-(\mathbf{p_2}) - \pi^-(\mathbf{p_1})\pi^+(\mathbf{p_2})]\,, \quad \mathbf{p_1} + \mathbf{p_2} = \mathbf{P}\,,\\ \pi^\pm(\mathbf{p_i}) &= \sum_{\mathbf{x}} e^{i\mathbf{p_i}\mathbf{x}}\, \bar{q}\gamma_5\tau^\pm q\,(t, \mathbf{x}) \end{aligned}\quad (4)$$

In practice, the $\pi\pi$ interpolator is the most important among our 16 interpolators, since it couples to the scattering state much better than the quark-antiquark interpolators. Let us note that all other lattice studies aimed at Γ_ρ used at most one quark-antiquark and one $\pi\pi$ interpolator, which may not always allow for reliable extraction of the first excited energy level E_2.

Given the 16 interpolators, we compute the 16×16 correlation matrix $C_{ij}(t_f, t_i)$ for all initial and final time-slices $t_i, t_f = 1, .., N_T = 32$. The needed Wick contractions that enter the correlation matrix with our $\bar{q}q$ and $\pi\pi$ interpolators are depicted in Fig. 2. The contributions (a,c,e) in Fig. 2 cannot be evaluated solely from the quark propagator from one point $(t_i, \mathbf{x_i})$ to all other points of the lattice (such a propagator allowed most of the spectroscopy studies in the past). The contributions (a,c,e) require the propagators from all and to all points on the lattice, which is too costly to evaluate in practice. We use the recently proposed distillation method for this purpose [9], which enables the exact computation of the required contractions.

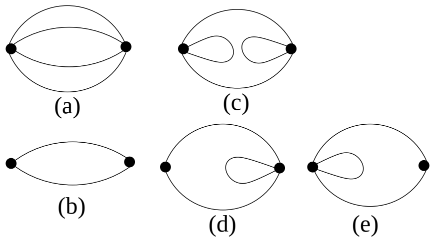

Fig. 2. Contractions for $I = 1$ correlators with $\bar{q}q$ (3) and $\pi\pi$ (4) interpolators.

P	level n	$E_n\,a$	$s\,a^2$	δ
$\frac{2\pi}{L}(0,0,0)$	1	0.5107(40)	0.2608(41)	130.56(1.37)
$\frac{2\pi}{L}(0,0,0)$	2	0.9002(101)	0.8103(182)	146.03 (6.58) [*]
$\frac{2\pi}{L}(0,0,1)$	1	0.5517(26)	0.1579(29)	3.06 (0.06)
$\frac{2\pi}{L}(0,0,1)$	2	0.6845(49)	0.3260(69)	156.41(1.56)
$\frac{2\pi}{L}(1,1,0)$	1	0.6933(33)	0.1926(49)	6.87(0.38)
$\frac{2\pi}{L}(1,1,0)$	2	0.7868(116)	0.3375(191)	164.25(3.53)

Table 1. The results for two lowest levels $n = 1, 2$ of the coupled $\pi\pi - \rho$ system with three choices of total momentum **P** on our lattice with $m_\pi a = 0.1673 \pm 0.0016$, $L = 16a$ and the lattice spacing $a = 0.1239 \pm 0.0013$ fm. The energy levels E_n are obtained by multiplying $E_n\,a$ with $a^{-1} \simeq 1.6$ GeV. The invariant mass squared of the system is $s = E_n^2 - \mathbf{P}^2$, but the dimensionless value in the table $s\,a^2$ is obtained using the discretized version of this relation [6].

We average the resulting correlators (i) over all initial time slices t_i at fixed time separation $t_f - t_i$, (ii) over all directions of momenta **P** (1) and (iii) over all directions of the ρ meson polarization.

The time dependence $t_f - t_i$ of the correlators $C_{ij}(t_f, t_i)$ (2) contains the information on the energies of the system E_n, and several methods for extracting E_n from C_{ij} are available. We extract two lowest energy levels $E_{n=1,2}$ of the system from the 16×16 correlation matrix $C_{ij}(t_f, t_i)$ using the so called variational method [10], which is the most established among the available methods. Table 1 displays the extracted lowest two energies $E_{n=1,2}$ of the coupled $\pi\pi - \rho$ system for our three choices of total momenta **P** (1).

The spectrum E_n in Table 1 for our finite box is the main result of this section. Each energy level corresponds to a different value of $s = E_n^2 - \mathbf{P}^2$, as calculated from E_n and **P** in the Table 1. In fact, the table lists values of s obtained from the discrete lattice version of the dispersion relation, which takes into account part of the corrections to $s = E_n^2 - \mathbf{P}^2$ due to finite lattice spacing [6].

3 Extraction of the phase shifts from energy levels

Let us consider the case when the resonance R can strongly decay only to two spinless hadrons H_1 and H_2, so one has elastic scattering of H_1 and H_2. We point out that the non-elastic case, when a resonance can decay strongly to several final states (i.e. H_1H_2 and $H_1'H_2'$), is much more challenging for a lattice study.

Suppose one encloses two hadrons $H_1(p_1)$ $H_2(p_2)$ with three-momenta p_1 and p_2 into a large box of size $L \gg$ fm and measures their energy. In a large box, they hardly interact and their energy is equal to sum of individual energies $E^{non-int} = E_{H1}(p_1) + E_{H2}(p_2)$ with $E_H(p) = \sqrt{m_H^2 + p^2}$. Now, let's force $H_1(p_1)$ and $H_2(p_2)$ to interact by decreasing the size of the box to L of a few fm. The energy of the system $E(L) = E_{H1}(p_1) + E_{H2}(p_2) + \Delta E(L)$ is shifted with respect to $E^{non-int}$: it will increase ($\Delta E(L) > 0$) if the interaction is repulsive and decrease ($\Delta E(L) < 0$) if the interaction is attractive. This simple physical reasoning indicates that the energy shift $\Delta E(L)$ gives info on the interaction.

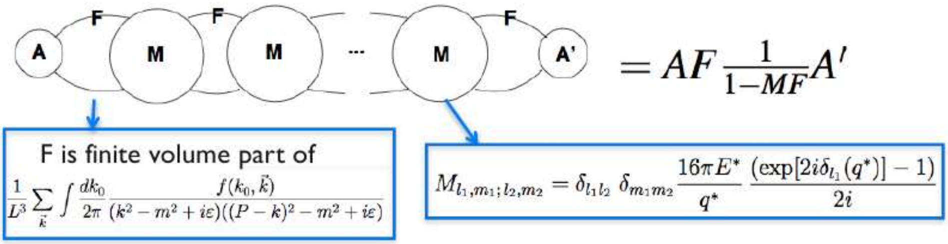

Fig. 3. The scattering of two interacting particles as series of the interaction vertex $M(\delta_L)$ and the scattering of non-interacting particles F at finite L [11].

In fact, the energy shift $\Delta E(L)$ and the energy itself $E(L)$ do not only give us "some" info on the interaction. According to the seminal analytic work of Lüscher [1], $E(L)$ or $\Delta E(L)$ rigorously tells us the value of the elastic scattering phase shift of H_1H_2 scattering at $L \to \infty$, i.e. $\delta(L = \infty)$:

$$\text{Luscher method}: \qquad E(L) \longrightarrow \delta(s, L=\infty) \qquad s = E(L)^2 - \mathbf{P}^2 \tag{5}$$

The derivation and the resulting formulae between $E(L)$ and δ are lengthy and rather complicated, but let us briefly explain at least why $E(L)$ contains info on $\delta(L = \infty)$. A nice and clear quantum-filed theory derivation is given in [11] and the main message is illustrated in Fig. 3. The scattering of two interacting spinless hadrons H_1H_2 at finite L (for degenerate case $m_{H1} = m_{H2} = m$) is represented in QFT by series of:

- scattering of two non-interacting hadrons at finite L, represented by F. The expression F contains sums over the loop momenta $\mathbf{k}$, which are allowed in a finite box L with periodic boundary conditions in space. Here $f(k_0, \mathbf{k})$ stands for dependence of the vertices on the left and right on k_0 and $\mathbf{k}$.

- the interaction vertex M with four hadron legs. This vertex depends on the elastic phase shift δ_l (at infinite volume) for the case of elastic scattering in the l-th partial wave.

The physical scattering requires resummation of the bubbles in Fig. 3, with non-interacting parts F and the interacting parts M, giving $AF\frac{1}{1-MF}A'$. The positions of the poles of the sum $AF\frac{1}{1-MF}A'$ obviously depend on M and therefore on δ_l. The positions of the poles dictate the possible energy levels of the system $E_n(L)$, so the energy levels $E_n(L)$ depend on M and therefore on δ_l.

The purpose of the above illustration was just to indicate why $E_n(L)$ depend on δ_l. In the case of $\pi\pi$ with $J^P = 1^-$, the relevant wave has $l = 1$ and we denote the corresponding phase by $\delta \equiv \delta_1$. The complete analytic relations between $E_n(L)$ and $\delta(s)$ needed for our case of the $\pi\pi$ scattering with $J^{PC} = 1^{--}$ and $I = 1$ are provided in [6] (for every $|\mathbf{P}|$ a different form of relation applies). These allow to extract δ for each of our six energy levels in Table 1 and the resulting phase shifts are given in the same Table.

The presented Lüscher formalism applies only for the case of elastic scattering. The $\pi\pi$ state is the only scattering state in this channel for energies when 4π state cannot be created, i.e., when $s = E_n^2 < (4m_\pi)^2$. For our $m_\pi a = 0.1673$ this is valid for all six levels, with the exception of the level E_1 at $\mathbf{P} = 0$, which is above 4π inelastic threshold. As the Lüscher analysis is not valid above the inelastic threshold, we omit this level from further analysis.

The resulting scattering phase shifts for five values of s are shown in Fig. 4. This is the main result of the lattice study; the resonance properties will be obtained by fitting $\delta(s)$ in the next section.

Note that the resulting phases are determined with a relatively good precision, which is better than in other available lattice studies of ρ at comparable u/d quark masses. The good precision can be traced back to various advanced techniques we used: the distillation method for evaluating contractions, usage of a large interpolator basis and average over all initial time slices, directions of momenta $\mathbf{P}$ and polarizations of ρ.

4 Extracting resonance mass and width from the phase shift

The phase shift $\delta(s)$ in Fig. 4, obtained directly from the lattice study, can be used to extract the properties of the resonance, in our case the ρ. The phase shift has a typical resonance shape: it passes from $\delta \simeq 0°$ to $\delta \simeq 180°$: the point where it crosses $90°$ gives the position of the resonance ($s = m_\rho^2$), while the steepness of the rise gives its width Γ_ρ. In particular, δ is related to resonance parameters by expressing the scattering amplitude a_l in terms of δ on one hand, and with Breit-Wigner form in the vicinity of the resonance on the other hand

$$a_1 = \frac{-\sqrt{s}\,\Gamma(s)}{s - m_\rho^2 + i\sqrt{s}\,\Gamma(s)} = \frac{e^{2i\delta(s)} - 1}{2i}\ . \tag{6}$$

Relation (6) can be conveniently re-written as

$$\sqrt{s}\,\Gamma(s)\ \cot\delta(s) = m_\rho^2 - s\ . \tag{7}$$

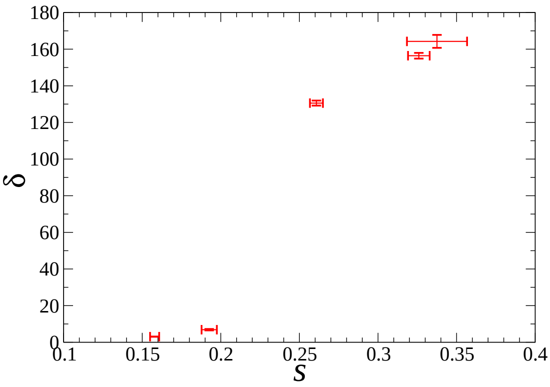

Fig. 4. The $\pi\pi$ phase shift $\delta(s)$ (in degrees) for five different values of dimensionless $sa^2 = (E_n a)^2 - (\mathbf{P}a)^2$, extracted from our lattice study [6]. The s is obtained by multiplying sa^2 with $(a^{-1})^2 \simeq (1.6\ \text{GeV})^2$.

	lattice (this work [6]) $m_\pi \simeq 266$ MeV	exp [PDG]
m_ρ	792 ± 12 MeV	775 MeV
$g_{\rho\pi\pi}$	5.13 ± 0.20	5.97

Table 2. Our lattice results for the resonance parameters [6], compared to the experimental values.

The decay width significantly depends on the phase space and therefore on m_π, so the decay width extracted at $m_\pi \simeq 266$ MeV could not be directly compared to the measured width. So, it is customary to extract the $\rho \to \pi\pi$ coupling $g_{\rho\pi\pi}$ instead of the width, where the width

$$\Gamma(s) = \frac{p^{*3}}{s}\frac{g_{\rho\pi\pi}^2}{6\pi}\ , \qquad \Gamma_\rho = \Gamma(m_\rho^2) \tag{8}$$

depends on the phase space for a P-wave decay and the coupling $g_{\rho\pi\pi}$. The coupling is expected to be only mildly dependent on m_π, which was explicitly confirmed in the lattice studies [5,7] and analytic study [12]. In (8), p^* denotes the pion momentum in the center-of-momentum frame and we extract it from s using a discretized version of relation $\sqrt{s} = 2\sqrt{m_\pi^2 + p^{*2}}$ [6]. Inserting $\Gamma(s)$ (8) into (7), one obtains an expression for $\delta(s)$ in terms of two unknown parameters: m_ρ and $g_{\rho\pi\pi}$. We fit these two parameters using five values of $\delta(s)$ given in Fig. 4 and Table 1, and we get the values of resonance parameters in Table 2 with small statistical errors.

The resulting ρ-meson mass in Table 2 is slightly higher than in experiment, as expected due to $m_\pi = 266\ \text{MeV} > m_\pi^{exp}$. The coupling $g_{\rho\pi\pi}$ is rather close to the value $g_{\rho\pi\pi}^{exp}$ derived from the experimental width Γ_ρ^{exp}.

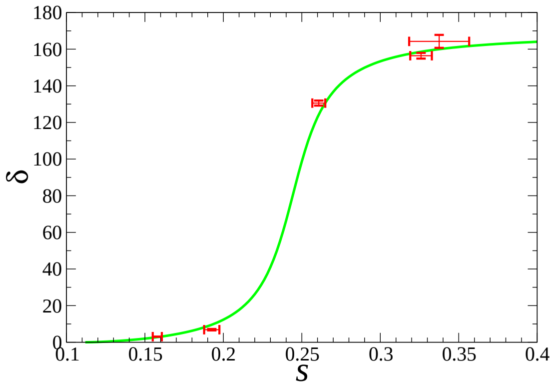

Fig. 5. The crosses are the $\pi\pi$ phase shift $\delta(s)$ (in degrees) for five different values of dimensionless $sa^2 = (E_n a)^2 - (\mathbf{P}a)^2$, extracted from our lattice study [6]. The line is the Breit-Wigner fit (7,8) for the resulting m_ρ and $g_{\rho\pi\pi}$ in Table 2. The physical value of s is obtained by multiplying sa^2 with $(a^{-1})^2 \simeq (1.6\ \mathrm{GeV})^2$.

5 Comparison to other lattice and analytical studies

The comparison of our results for m_ρ and Γ_ρ to two recent lattice studies [5, 7] is compiled in Fig. 8 of [7]. Our result has the smallest error on a given ensemble, demonstrating that accurate lattice determination m_R and Γ_R for (some) resonances is possible now. The other two lattice studies are done for two [7] and four [5] pion masses and explicitly demonstrate mild dependence of $g_{\rho\pi\pi}$ on m_π. The discussion concerning the (dis)agreement of the three lattice studies is given in [7] and will be extended in [13].

The comparison of our $\delta(s)$ to the prediction of the lowest non-trivial order of unitarized Chiral Perturbation Theory [14] is given by the solid line in 6, which has been recalculated for our $m_\pi = 266$ MeV in [15]. The lowest[1] order prediction does not depend on unknown LECs and agrees reasonably well with our lattice result, given by the bullets.

6 Conclusions

We highlighted the main physical reasoning, which lies behind the lattice extraction of elastic phase shifts $\delta(s)$ and the resonance parameters m_R and Γ_R. The purpose was to present the general principle of the method and omit the technical details. The method was presented on the example of $\pi\pi \to \rho \to \pi\pi$ scattering. This example demonstrates that a proper first-principle treatment of some hadronic resonances on the lattice is now possible.

[1] One cannot make a fair comparison between out lattice result and the next-to-lowest order prediction, since it depends on a number of LECs, and some of them have been fixed using m_ρ from another lattice study, which gets a significantly higher m_ρ.

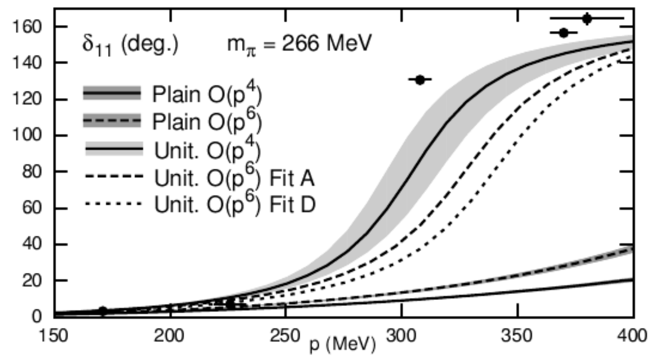

Fig. 6. The $\pi\pi$ phase shift in the ρ channel $\delta_{11}(p) \equiv \delta(p^*)$ at $m_\pi = 266$ MeV: the solid line (indicated by "Unit $O(p^4)$") gives prediction of the lowest order of Unitarized Chiral Perturbation Theory [14, 15], while bullets are our lattice data.

Acknowledgments We would like to kindly thank Anna Hasenfratz for providing the gauge configurations used for this work. We would like to thank Xu Feng, Naruhito Ishizuka, Jose Pelaez, Gerrit Schierholz and Richard Woloshyn for valuable discussions. The calculations have been performed on the theory cluster at TRIUMF and on local clusters at the University of Graz and Ljubljana. We thank these institutions for providing support. This work is supported by the Slovenian Research Agency, by the European RTN network FLAVIAnet (contract number MRTN-CT-035482) and by the Natural Sciences and Engineering Research Council of Canada (NSERC).

References

1. M. Lüscher, Commun. Math. Phys. 105 (1986) 153; Nucl. Phys. B 354 (1991) 531; Nucl. Phys. B 364 (1991) 237.
2. S. Aoki *et al.*, CP-PACS coll., Phys. Rev. D 76 (2007) 094506.
3. M. Göckeler *et al.*, QCDSF coll., PoS LAT (2008) 136, arXiv:0810.5337.
4. J. Firson *et al.*, BMW coll., arXiv:1011.3413.
5. X. Feng, K. Jansen and D.B. Renner, Phys. Rev. D (2011) 094505.
6. C.B. Lang, D. Mohler, S. Prelovsek and M. Vidmar, Phys. Rev. D 84 (2011) 054503, arXiv:1105.5636.
7. S. Aoki *et al.*, PACS-CS coll., arXiv:1106.5365.
8. A. Hasenfratz *et al.*, Phys. Rev. D 78 (2008) 054511, Phys. Rev. D78 (2008) 014515.
9. M. Peardon *et al.*, Phys. Rev. D 80 (2009) 054506, arXiv:0905.2160.
10. M. Lüscher and U. Wolff, Nucl. Phys. B 339 (1990) 222; B. Blossier *et al.*, JHEP 0904 (2009) 094, arXiv:0902.1265 [hep-lat]
11. C. Kim, C. Sachrajda and S. Sharpe, Nucl. Phys. B727 (2005) 218, hep-lat/0507006.
12. J. Pelaez and G. Rios, Phys. Rev. D 82 (2010) 114002, arXiv:1010.6008.
13. C.B. Lang, D. Mohler and S. Prelovsek, to be prepared for the LAT2011 proceedings.
14. J. Nebreda, J.R. Pelaez and G. Rios, Phys. Rev. D 83 (2011) 094011, arXiv:1101.2171;
15. J. Nebreda, J. R. Pelaez and G. Rios, arXiv:1108.5980

BLED WORKSHOPS
IN PHYSICS
VOL. 12, NO. 1
p. 82

Proceedings of the Mini-Workshop
Understanding hadronic spectra
Bled, Slovenia, July 3 - 10, 2011

The pion cloud of the nucleon in the constituent quark picture *

Bogdan Povh[a] and Mitja Rosina[b,c]

[a]Max-Planck-Institut für Kernphysik, Postfach 103980, D-69029 Heidelberg, Germany
[b]Faculty of Mathematics and Physics, University of Ljubljana, Jadranska 19, P.O. Box 2964, 1001 Ljubljana, Slovenia
[c]J. Stefan Institute, 1000 Ljubljana, Slovenia

Abstract. The importance of the pion cloud in the nucleon has been demonstrated in the study of the magnetic polarizabilities, electroexcitation, spin properties of the nucleon and, more recently, in deep inelastic scattering. The model in which the pion cloud of the nucleon is generated by the $qq\bar{q}$ component in the constituent quark has been successful in explaining the spin properties and the flavor asymmetric sea of the nucleon. We show that the same parameters yield the pion in $p \to n\pi^+$ and $p \to p\pi^0$ fluctuation in agreement with the observed value in the ($e + p \to e+$ forward neutron+X) experiment.

1 Introduction

First we review some evidence for the role of the pion cloud in explaining nucleon observables. As examples of low-energy processes, we quote the magnetic polarizabilities [1] and electroexcitation of the nucleon [2–4]. The pion cloud acts as a coil and gives a diamagnetic contribution while the virtual excitation of the N-like quark core into the Δ-like quark core acts as a paramagnet. The magnetic polarizability of the nucleon results from an approximate cancellation between these two contributions. Without the pion cloud, the paramagnetic contribution would dominate and give much too large magnetic polarizability. In the electroexcitation of the nucleon into Δ and into the Roper resonance, the linear σ-model with quarks and the cloudy bag model help us understand why (40 - 50)% of the dominant M1 ampliutude and 100% of the E2 amplitude is due to pion cloud.

The question arises, whether the same amplitude of the pion cloud (or equivalently, the same probability of pion fluctuation) can explain also observables measured at higher energies where the stucture functions of quarks play a role and pion is seen through its contribution to the corresponding quark and antiquark structure function.

2 Pion cloud in quarks can explain nucleon observables

The notion of the constituent quark applies generally to the massive quark dressed by gluons, the constituent of the nucleon. This non-relativistic model with three

* Talk delivered by M. Rosina

massive constituent quarks works well for the hadronic masses and the magnetic moments. It breaks down if the spin properties of the baryons are considered. The improved version, the chiral constituent quark model is surprisingly succesful in explaining the spin properties of nucleons and hyperons. In the simplest form applied to the nucleon the chiral constituent quark is composed of a massive quark accompanied by a quark-antiquark pair coupled to the spin-parity quantum numbers of the pion $J^{\pi} = 0^{-}$. In the following we write the pion symbol as a shortcut to the quark-antiquark pair coupled to the pion quantum numbers. This simple model has been first applied by Eichten et al. [5] to explain the flavor asymmetry of the sea quarks and further elaborated by Baumgärtner et al. [6] and Pirner [7] in the interpretation of the spin properties of the nucleon. It is related to the three-flavour extension proposed by Cheng and Li [8]. Explicitly written, the chiral constituent up-quark (u) structure is

$$|u\rangle = \sqrt{(1 - \frac{3}{2}\,a)}\,|\mathbf{u}\rangle - \sqrt{a}|\mathbf{d}\pi^{+}\rangle + \sqrt{\frac{a}{2}}\,|\mathbf{u}\pi^{0}\rangle, \tag{1}$$

and of the down quark (d)

$$|d\rangle = \sqrt{(1 - \frac{3}{2}\,a)}\,|\mathbf{d}\rangle + \sqrt{a}\,|\mathbf{u}\pi^{-}\rangle - \sqrt{\frac{a}{2}}\,|\mathbf{d}\pi^{0}\rangle. \tag{2}$$

The basis of pure flavour quarks is denoted by boldface **u** and **d**.

At $Q^2 \approx 0$ gluons do not appear as an explicit degree of freedom and the nucleon is composed of quarks and quark-antiquark pairs. Thus in the lowest order the Fock state of the constituent quark has the form (1 and 2), where in the second and third term the quark-antiquark pair is coupled to the $J^{\pi} = 0^{-}$ quantum nummbers of the pion. This simple structure of the chiral constituent quark (1) has two attractive features. Firstly, as we will show, the chiral constituent quark reproduces the experimental results of the deep inelastic scattering and axial-vector beta decays of the neutron quantitatively; secondly, this model complies with our picture of the origin of the quark mass by the chiral symmetry breaking mechanism of Nambu and Jona-Lasino [9]. Dressing the light quark by gluons is inevitably accompanied by creation of the Goldstone boson, the pion. The Goldstone pion is an inherent part of the constituent quark.

The parameter a of (1, 2) is usually determined from the value of the axial vector coupling constant $g_A = 1.269 \pm 0.003$ [11] yielding $a = 0.239 \pm 0.002$. The parameter a measures the probability of the constituent quark to be in the state accompanied with a charged pion. Furthermore, with the probability $a/2$ the constituent quark is in a state component with the neutral pion. Thus the total probability of finding a pion in the constituent quark amounts thus to slightly more than one third. The large probability of the pion in the constituent quark is best manifested in the measurements of the quark polarization in the deep inelastic scattering. Not only that one third of the constituent quark with the pion does not contribute to the spin polarization, but even more, with the oppositely oriented quarks reduces the total quark polarization to one third of what would be without the pions. The loss of the angular momentum because of the oppositely oriented quark is compensated by the orbital angular momentum of the pion in the p-state. The comparison of the experimental results of the deep inelastic scattering with the prediction of the chiral constituent-quark model is given in [10]. It is also worthwhile to mention that the valence-quark distribution does not peak at Bjorken $x = 0.3$ but it is softer and peaks at $x = 0.2$ corresponding to five and not three constituts of the proton even before gluons can get excited. Eichten et al. ([5]) ascribe these quark-antiquark pairs to an asymmetric sea.

We consider also other observables which depend strongly on the pions in the nucleon: the Gottfried sum rule I_G (with corrections discussed in [10]), the integrals of the spin structure functions of proton I_p and deuteron I_d and the quark spin polarization $\Delta\Sigma$ [12,13]. They have larger error bars than g_A, but they agree reasonably well eith the model (Table 1.). The new experimental value for $\Delta\Sigma$ supports even more our assumption that the main contribution to the spin reduction comes from the pion fluctuation.

observable	model value	
$g_A = 1.269 \pm 0.003$	$\frac{5}{3}(1-a)$	$=$ input
$I_G = 0.216 \pm 0.033$	$\frac{1}{3}(1-2a)$	$= 0.174 \pm 0.002$
$I_p = 0.120 \pm 0.017$	$\frac{5}{18}(1-2a)$	$= 0.145 \pm 0.002$
$I_d = 0.043 \pm 0.006$	$\frac{5}{36}(1-3a)$	$= 0.039 \pm 0.001$
$\Delta\Sigma = 0.330 \pm 0.064$	$(1-3a)$	$= 0.283 \pm 0.006$

Table 1. The π^+ probability $a = 0.239 \pm 0.002$ is used to calculate different observables

3 The proton contains a neutron plus pion component

Let us consider the matrix element $\langle n\pi^+|p\rangle$.

Inserting for constituent quarks our chiral quarks it is evident that the $\langle n\pi^+|$ has an overlapp with a Fock component of the proton. The result of the explicit calculation is

$$|\langle n\pi^+|p\rangle|^2 = |\langle d\pi^+|u\rangle|^2 = (1 - \frac{3}{2}\,a)\,a = 0.15. \tag{3}$$

The result (3) means that the constituent u quark has a component of the d quark and a pion. Although the proton has two u quarks there is no factor 2 in the amplitude, due to the flavor-spin-color structure of the nucleon. The flavor-spin wavefunction of the proton has a mixed symmetry combined into a symmetric flavor-spin function:

$$|p\rangle = \sqrt{\frac{1}{2}}\;\begin{array}{|c|c|}\hline 1 & 2 \\ \hline 3 & \multicolumn{1}{c}{} \\ \cline{1-1}\end{array}_{\,f} \times \begin{array}{|c|c|}\hline 1 & 2 \\ \hline 3 & \multicolumn{1}{c}{} \\ \cline{1-1}\end{array}_{\,s} + \sqrt{\frac{1}{2}}\;\begin{array}{|c|c|}\hline 1 & 3 \\ \hline 2 & \multicolumn{1}{c}{} \\ \cline{1-1}\end{array}_{\,f} \times \begin{array}{|c|c|}\hline 1 & 3 \\ \hline 2 & \multicolumn{1}{c}{} \\ \cline{1-1}\end{array}_{\,s}\,. \tag{4}$$

A similar expression stays for the neutron. Since the combined wavefunction is symmetric under all permutations it is enough to look at the contribution of the particles 1 and 2. In the first term of the proton wavefunction the particles 1 and 2 are symmetric and can both be u quarks and contribute constructively to the matrix element with a factor of two. In the second term the interference is destructive and the contribution cancels. Thus only the first term contributes to the matrix element. Since both in proton and in neutron the first term appears with a factor $\sqrt{1/2}$, the factor two is canceled out. This qualitative explanation can be verified by writing down the three-quark wavefunctions explicitly.

This can be seen even easier in the isospin formalism. In the act of producing a positive pion, the corresponding u quark loses one unit of charge, it becomes a d quark. This can be described with the operator $\sum_i t_-(i) = T_-$ where $T_- = T_x - iT_y$. We conveniently took the sum over all three quarks since the third quark, d, contributes zero anyway. The expectation value is $< TM-1|T_-|TM >= \sqrt{T(T+1)-M(M-1)}$ which for proton $(T = 1/2, M = 1/2)$ gives in fact the factor 1. It is instructive to compare with Δ^+ $(T = 3/2, M = 1/2)$ in the process ep$\rightarrow$ eΔX where one gets the factor 2, pointing out that the two u quarks are always symmetric and interfere constructively. Of course, for the squared amplitude, we get the additional factor a since only the π^+-dressed component of the u-quark contributes, and the factor $(1-\frac{3}{2}a)$ for the naked component of the final d-quark.

4 Experimental test of the pion fluctuation

The pion fluctuation of nucleon is well known in the classical nuclear physics as anomalously large pion-nucleon coupling constant $g^2/4\pi = 13.6$. Many of the nucleon properties are ascribed to the pion cloud of the nucleon [14]. Hovewer, there is no direct way of determinig experimentally the probability of finding a pion fluctuation in the proton. The best way is to calculate the pion flow by using the pion-nucleon coupling constant and the form factor assuming that the pion is emitted by a proton [15], [16]

$$f_{\pi^+/p}(x_L,t) = \frac{1}{2\pi}\frac{g^2_{p\pi n}}{4\pi}(1-x_L)^{1-2\alpha(t)}\frac{-t}{(m_\pi^2-t)^2}|G(t)|^2. \tag{5}$$

The pion flow is related to the measured cross section by

$$\mathbf{d}\sigma^{\gamma^* p\rightarrow nX} = f_{\pi^+/p}(x_L,t)\cdot \mathbf{d}\sigma^{\gamma^*\pi^+\rightarrow X} \tag{6}$$

where the $(\gamma^*\pi^+ \rightarrow X)$ DIS cross section is assumed to be 2/3 of the $(\gamma^* p \rightarrow X)$ DIS cross section in the cited analysis, with corrections due to absorption [10].

Obviously the pion is not emitted by a proton but by a quark. But as we showed above the state of the pion is dictated by the proton wave function and the pion form factor simulated well the assumption that the emission is from the proton. In the series of experiments [17]- [18], [19] measuring the spectrum of the forward neutrons in the reaction (e+p$\rightarrow$e+forward n+X) has been shown that the high energy end of the neutron spectrum is consistent with the assumption that the deep inelastic scattering takes place on the pion. Thus we are justified to say that the forward neutron is the signature of the reaction taking place on the pion and that the total probability of finding a pion in ep$\to$nπ^+ fluctuation can be obtained by integrating over the variables of the pion flow.

The analysis depends to some extent on the estimation of pion flux $f_{\pi^+/p}$. The analysis has been elaborated in [10] and the quoted results are $\langle n\pi^+|p\rangle^2 = 0.165 \pm 0.01$ and 0.175 ± 0.01, respectively, for the two form factors best fitting to the experiment in [15] and [16].

5 Conclusion

The pion fluctuation p$\to$n+π^+ and p$\to$p+π^0 is an artifact of the quark-antiquark pairs of the constituent quarks. The impressive agreement between the measured and the calculated ratios between the probability of the pion fluctuation and the probability of finding a quark-antiquark pair of the constituent quark is a strong support of the constituent quark model.

In this section we stress the difference between the notion of the quark-antiquark pairs coupled to the pion quantum numbers being part of the constituent quarks and the pions of the proton. While the quark-antiquark pairs are implied by the experimental values of g_A, the integrated spin structure functions and the violation of the Gottfried summ rule, the fluctuating pions are identified by the characteristic energy and p_T distribution of the neutron spectra in the ep $\to$ nπ^+ reaction.

Eichten et al. [5] have named the quark-antiquark pairs of the constituent quark the asymmetric quark sea. This name emphasizes hopefully sufficiently the difference of their origin as compared to the normal quark sea.

For the value $a = \langle \mathbf{d}\pi^+|u\rangle^2 = 0.24$ each quark contains 0.36 quark-antiquark pairs. Summing up the quark-antiquark pairs one obtains about one quark-antiquark pair per nucleon. Using this value of a gives $\langle n\pi^+|p\rangle^2 = 0.15$. This number corresponds well with the experimental value of $\langle n\pi^+|p\rangle^2 = 0.165 \pm 0.01$ or 0.175 ± 0.01. It follows that in ≈ 0.26 cases the proton is a neutron+ π^+ or a proton+π^0. This means that about one quater of the nucleon's quark-antiquark pairs show up as the pion fluctuation.

Acknowledgments We wish to thank A. Bunyatyan for the discussions of the analysis on the forward neutron spectra and K. Rith for pointing us out the new results on spin-polarization data in DIS.

References

1. B. Golli and R. Sraka, Phys. Lett. B **312** (1993) 24-29.
2. M. Fiolhais, B. Golli and S. Širca, Phys. Lett. B **373** (1996) 229-234.
3. B. Golli and S. Širca, Eur. Phys. J. A **38** (2008) 271-286.
4. B. Golli, S. Širca and M. Fiolhais, Pion electro-production in the Roper region in chiral quark models, Eur. Phys. J. A **42** (2009) 185-193.
5. E.J.Eichten, I.Hinchliffe and C.Quigg, Phys. Rev. D **45** (1992) 2269.

6. S. Baumgaertner, H. J. Pirner, K. Koenigsmann, B. Povh, Z. Phys. A **353** (1996) 397.
7. H. J. Pirner, Prog. Part. Nucl. Phys. **36** (1996) 19-28.
8. T. P. Cheng and Ling-Fong Li, Phys. Rev. Lett. **74** (1995) 2872-2875.
9. S.P. Klevansky, Rev. Mod. Phys. **64** (1992) 694.
10. A. Bunyatyan and B. Povh, Eur. Phys. J. A **27** 2006 359-364.
11. K. Nakamura et al. (Particle Data Group), J. Phys. G **37** (2010) 075021.
12. K. Rith, Prog. Part. Nucl. Phys. **49** (2002) 245.
13. A. Airapetian et al., Phys. Rev. D **75** (2007), 012007.
14. A. W. Thomas, Prog. Theor. Phys. **168** (2007) 614
15. B. Kopeliovich, B. Povh and I. Potashnikova, Z. Phys. C **73** (1996) 125, [hep-ph/9601291].
16. H. Holtmann *et al.*, Phys. Lett. B **338** (1994) 363.
17. C. Adloff *et al.* [H1 Collaboration], Eur. Phys. J. C **6** (1999) 587, [hep-ex/9811013].
18. A. Aktas *et al.* [H1 Collaboration], Eur. Phys. J. C **41** (2005) 273, [hep-ex/0501074].
19. S. Chekanov *et al.* [ZEUS Collaboration], Phys. Lett. B **610** (2005) 199, [hep-ex/0404002], and references therein.